

Article

Tin Complexes Derived from the Acids $\text{Ph}_2\text{C}(\text{X})\text{CO}_2\text{H}$ ($\text{X} = \text{OH}$, NH_2): Structure and ROP Capability

Timothy J. Prior  and Carl Redshaw * 

Plastics Collaboratory, Chemistry, School of Natural Sciences, University of Hull, Cottingham Road, Hull HU6 7RX, UK; t.prior@hull.ac.uk

* Correspondence: c.redshaw@hull.ac.uk

Abstract: Interaction of $[\text{Sn}(\text{O}t\text{Bu})_4]$ with the acid 2,2'-diphenylglycine, $\text{Ph}_2\text{C}(\text{X})\text{CO}_2\text{H}$ ($\text{X} = \text{NH}_2$), affords the complex $\{\text{Sn}[\text{Ph}_2\text{C}(\text{NH}_2)(\text{CO}_2)]_4\} \cdot 2\text{MeCN}$ (**1**·2MeCN) after work-up, whereas when $\text{X} = \text{OH}$ (benzoic acid), the complex $\{\text{Sn}[\text{Ph}_2\text{C}(\text{O})(\text{CO}_2)]_2(\text{CH}_3\text{CO}_2\text{H})_2\}$ (**2**) is isolated. In **1**·2MeCN, the four 2,2'-diphenylglycinate ligands adopt three different coordination modes (two *N,O*-chelates, an *O,O*-chelate, and a monodentate carboxylate ligand), whilst in **2**, two *cis-O,O*-chelate ligands are present along with two acetic acid ligands, the latter being derived from hydrolysis of acetonitrile. Both **1** and **2** have been screened as catalysts for the ring opening polymerization of ϵ -caprolactone and δ -valerolactone; for comparison, the commercial catalyst $[\text{Sn}(\text{Oct})_2]$, where Oct = 2-ethylhexanoate, and the precursor $[\text{Sn}(\text{O}t\text{Bu})_4]$ have been screened under similar conditions. The products were of low to high molecular weight for PCL and low to moderate molecular weight for PVL, with wide Đ values, and they comprised several types of polymer families, including OH-terminated, OH/OMe-terminated, and cyclic polymers. For both monomers, kinetic profiles indicated that $[\text{Sn}(\text{Oct})_2]$ outperformed **1**, **2**, and $[\text{Sn}(\text{O}t\text{Bu})_4]$, though under certain conditions, **1** and **2** afforded high-molecular weight products with better control.

Keywords: tin complexes; Ph_2C -functionalized carboxylic acids; solid-state structures; ring opening polymerization (ROP); cyclic esters



Academic Editor: Soghomon Boghosian

Received: 29 January 2025

Revised: 25 February 2025

Accepted: 7 March 2025

Published: 9 March 2025

Citation: Prior, T.J.; Redshaw, C. Tin Complexes Derived from the Acids $\text{Ph}_2\text{C}(\text{X})\text{CO}_2\text{H}$ ($\text{X} = \text{OH}$, NH_2): Structure and ROP Capability. *Catalysts* **2025**, *15*, 261. <https://doi.org/10.3390/catal15030261>

Copyright: © 2025 by the authors. Licensee MDPI, Basel, Switzerland. This article is an open access article distributed under the terms and conditions of the Creative Commons Attribution (CC BY) license (<https://creativecommons.org/licenses/by/4.0/>).

1. Introduction

Petroleum-based plastics continue to be essential for a variety of everyday applications; however, the issues associated with global plastic pollution are driving the search for more environmentally friendly materials [1–3]. With this in mind, much research has focused on the ring opening polymerization (ROP) of cyclic esters. This process typically employs a catalyst, which can be either metal- or organic-based [4–12], and in the former case, the active species tends to be either a metal alkoxide or carboxylate. The other ancillary ligands bound to the catalytic metal centre also play a crucial role in controlling the local sterics and electronics of the system and can also greatly influence other properties such as solubility. Commercially, the catalyst of choice is tin octanoate, $[\text{Sn}(\text{Oct})_2]$, which was selected given its high catalytic activity (high reaction and conversion rates), ability to afford high-molecular weight products, and relatively low cost, despite the cytotoxicity associated with tin compounds [13]. There is considerable interest in the development of new tin-based catalysts for the ROP of cyclic esters [14–36]. For example, Limwanich et al. have recently investigated the microwave-assisted ROP of ϵ -caprolactone under solvent-free conditions using *n*-butyltin(IV) chlorides [36]. We have been investigating the coordination chemistry of the acids $\text{Ph}_2\text{C}(\text{X})\text{CO}_2\text{H}$, where $\text{X} = \text{NH}_2$ or OH [37–45],

given their ability to impart high crystallinity on subsequent products [46]. Given this, we have extended our studies of these acids to tin chemistry and report herein two products arising from the interaction of $\text{Ph}_2\text{C}(\text{X})\text{CO}_2\text{H}$, $\text{X} = \text{NH}_2, \text{OH}$, with $[\text{Sn}(\text{O}t\text{Bu})_4]$, Chart 1. $[\text{Sn}(\text{O}t\text{Bu})_4]$ was chosen as the entry point, despite the increased toxicity associated with Sn(IV), as solid Sn(II) alkoxides tend to suffer from solubility issues [32]. The tin products **1** and **2** have been screened for their ROP capability with the cyclic esters ϵ -caprolactone (ϵ -CL) and δ -valerolactone (δ -VL). Results are compared against the commercial catalyst $[\text{Sn}(\text{Oct})_2]$, where Oct = 2-ethylhexanoate, and the precursor $[\text{Sn}(\text{O}t\text{Bu})_4]$, which have been screened under the same conditions.

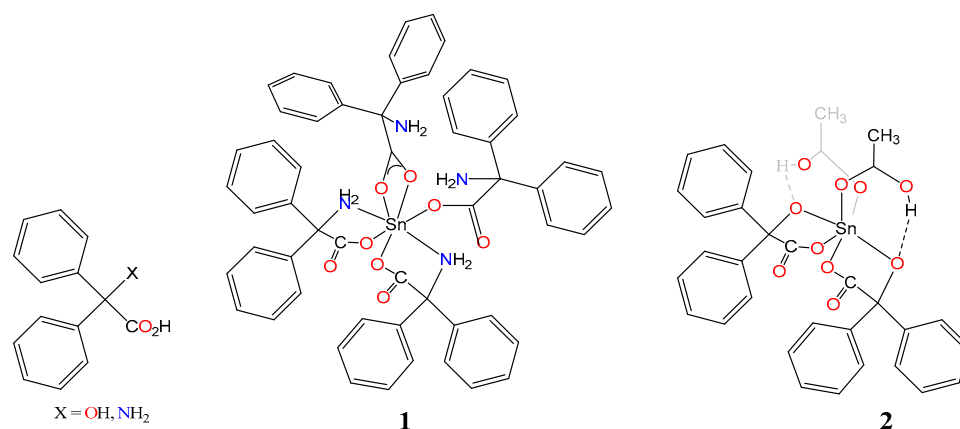


Chart 1. The acids $\text{Ph}_2\text{C}(\text{X})\text{CO}_2\text{H}$ ($\text{X} = \text{OH}, \text{NH}_2$) and the complexes **1** and **2**.

2. Results and Discussion

2.1. Diphenylglycine

Reaction of $[\text{Sn}(\text{O}t\text{Bu})_4]$ with $\text{Ph}_2\text{C}(\text{NH}_2)(\text{CO}_2\text{H})$, dpgH, in refluxing toluene afforded the complex $\{\text{Sn}[\text{Ph}_2\text{C}(\text{NH}_2)(\text{CO}_2)]_4\} \cdot 2\text{MeCN}$ (**1**·2MeCN) after work-up (extraction into MeCN). Single crystals suitable for X-ray diffraction were grown from a saturated MeCN solution on standing for 48h at 0 °C. The molecular structure is shown in Figure 1, with selected bond lengths and angles given in the caption; an alternative view of **1**·2MeCN is given in the Supplementary Materials (Figure S1). The complex crystallises in the centrosymmetric space group $P\bar{1}$ with a single, discrete tin complex in the asymmetric unit. The central Sn(VI) ion is seven-coordinate; four dpg^- anions are bound at the tin centre, but there are three different coordination modes. The first two dpg anions form five-membered chelates through the carboxylate and amine group (O1, N1 and O3, N2). This can be classified using the Harris notation [47] as a [1.011] binding mode. The third ligand binds through a chelating carboxylate (atoms O5 and O6) in mode [1.110]. The final ligand binds through a single oxygen of the carboxylate (O7). The different coordination modes are readily apparent from the carboxylate bond lengths. The assignment was greatly aided by excellent-quality difference Fourier maps which allowed for H-atoms to be identified. Hydrogens attached to carbon were fitted with a riding model; those attached to nitrogen were refined freely, subject to restraints that all N-H distances be the same with a standard deviation of 0.03 Å, and bond angles were similarly restrained. For the five-membered chelates, the C-O bond lengths are 1.308(3) and 1.216(3) Å for C1 and 1.298(3) and 1.216(3) Å for C15. The chelating carboxylate centred on C29 has C-O bond lengths of 1.282(3) and 1.245(3) Å. The strictly monodentate carboxylate centred on C43 has C-O bond lengths of 1.302(3) and 1.220(3) Å. There is very minor disorder in the position of one of the phenyl groups (two orientations in the ratio 0.569:0.431(15)), but this was modelled conservatively using standard techniques, involving bond length restraints for equivalent atoms in different disorder components. In addition to the tin complex, the asymmetric unit

contains two well-resolved molecules of acetonitrile which act as hydrogen bond acceptors to two NH₂ groups of the complex, forming a $D_1^1(2)$ hydrogen-bonding motif [48]. The phenyl rings are orientated in a propellor-like fashion, as noted for a number of benzilate complexes [49].

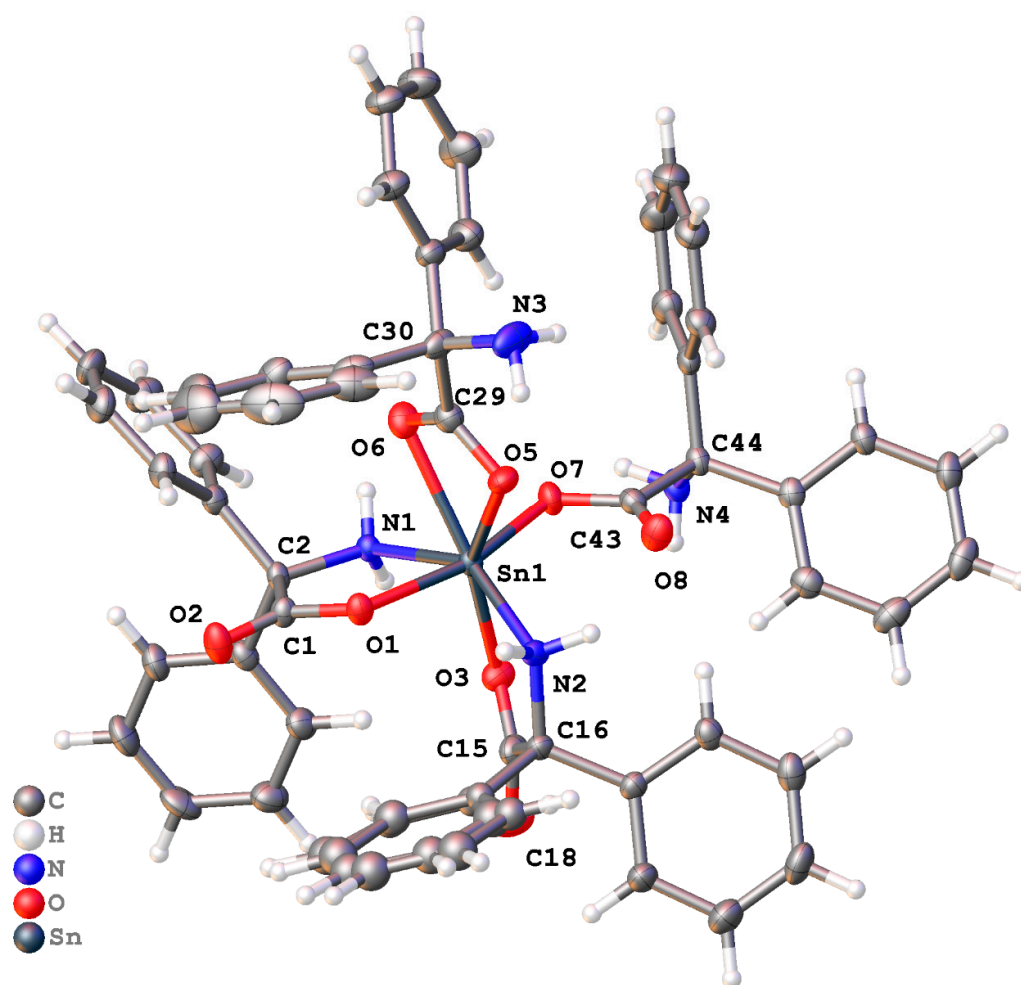


Figure 1. View of molecular structure of $\{[Sn(Ph_2C(NH_2)(CO_2)]_4 \cdot 2MeCN\}$ (1·2MeCN), drawn as 50% probability ellipsoids. For clarity, unbound solvent molecules have been omitted. Selected bond lengths (Å) and angles (°): Sn1—O1 2.0576(16), Sn1—O3 2.0923(18), Sn1—O5 2.1461(18), Sn1—O7 2.0687(16), Sn1—N1 2.2244(19), Sn—N2 2.2208(19); O1—Sn—N1 75.59(6), O3—Sn—N2 75.26(7), O5—Sn—O6 56.54(6), O1—Sn—O7 161.00(7).

There are no intramolecular hydrogen bonds. There is extensive N-H···N hydrogen bonding between adjacent molecules, but surprisingly, there are no N-H···O interactions. Most notably, adjacent molecules related by the inversion centre form an $R_2^2(14)$ embrace through N-H···N hydrogen bonds. There is also evidence for C-H···O interactions between adjacent molecules.

2.2. Benzilic Acid

Similar use of benzilic acid led to the complex $\{[Sn(Ph_2C(O)(CO_2)]_2(CH_3CO_2H)_2\}$ after work-up (MeCN) (2). Single crystals suitable for X-ray diffraction were grown from a saturated MeCN solution, standing for 48h at 0 °C. The molecular structure is shown in Figure 2, with selected bond lengths and angles given in the caption; an alternative view of 2 is given in the Supplementary Materials (Figure S2). The complex crystallises in the non-centric space group $I-42d$, with one half a complex in the asymmetric unit. There is minor disorder in the position of one of the phenyl groups (two orientations in the ratio

0.55:0.45(5)), but this was modelled conservatively using standard techniques, involving bond length restraints for equivalent atoms in different disorder components. Each Sn is six coordinate, and two doubly-deprotonated benzoic acid ligands form five-membered chelates to the Sn in a *cis* fashion. The remaining two coordination sites are completed by the carbonyl oxygen of acetic acid (C=O distance for the binding oxygen is 1.26(2) Å and for the C-OH, the C-O distance is 1.34(2) Å). The O-H group is not deprotonated but forms an intramolecular hydrogen bond to the carbonyl of the benzoic acid with motif $S_1^1(6)$. The crystal as a whole was found to contain a single enantiomer (Flack parameter 0.05(3)). The acetic acid ligand is thought to arise via the hydrolysis of MeCN; such a process usually occurs in the presence of an acid or base [50–52].

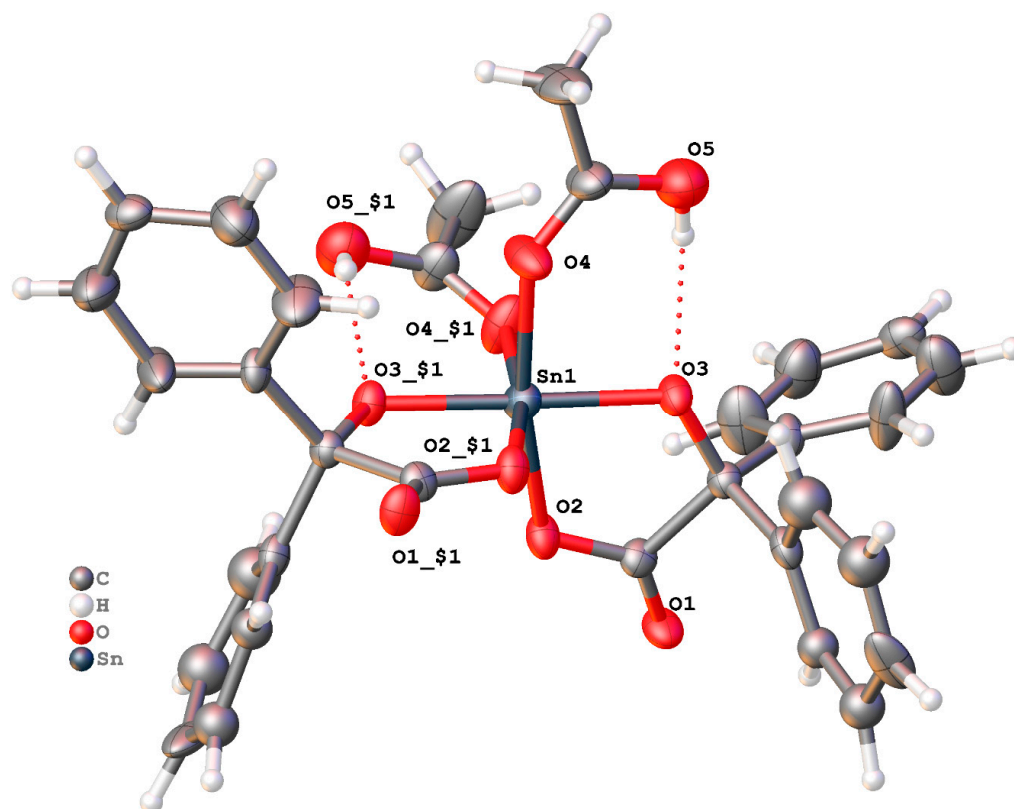


Figure 2. View of molecular structure of $\{\text{Sn}[\text{Ph}_2\text{C}(\text{O})(\text{CO}_2)]_2(\text{CH}_3\text{CO}_2\text{H})_2\}$, drawn as 30% probability ellipsoids. For clarity, minor disorder is not shown. Symmetry operation used to generate equivalent atoms: $x, 1.5-y, 1.25-z$. Selected bond lengths (Å) and angles ($^\circ$): Sn1—O2 2.044(10), Sn1—O3 1.965(8), Sn1—O4 2.073(10); O2—Sn—O3 81.6(4), O2—Sn—O4 169.7(4).

There is no included solvent in the structure despite the fact that four pockets of approximately 3.6% of the cell volume are present.

^1H NMR spectra for **1** and **2** are provided in the Supplementary Materials (Figures S3 and S4).

3. Ring Opening Polymerization (ROP)

3.1. Ring Opening Polymerization of ϵ -Caprolactone (ϵ -CL)

Complexes **1** and **2** have been screened for their ability to act as catalysts for the ROP of ϵ -caprolactone (ϵ -CL), and the results are presented in Table 1. Results for **1** and **2** are compared with the industrially employed catalyst $\text{Sn}(\text{Oct})_2$. For **1**, the ratio of $[\epsilon\text{-CL}]:[\text{Sn}]$ was varied between 100:1 and 1000:1 at 130 $^\circ\text{C}$ over 24 h under N_2 or air. Complexes **1** and **2** were found to be active under these polymerization conditions with

similar monomer conversions ($\geq 90\%$, except for entry 4 at 81%), affording polymers with moderate to relatively high molecular weights, with **1** under N_2 (entry 3, Table 1) affording the highest at *ca.* 48,750 Da, albeit with poor control ($\bar{D} = 3.81$); selected GPC traces are given in the Supplementary Materials (Figures S5–S11). Interestingly, consistent with the wide \bar{D} values, the MALDI-TOF spectra revealed several families of products, including OH-terminated polymers and cyclic polymers (e.g., Figures 3–6). There was evidence of transesterification, and all observed M_n values were significantly lower than the calculated values. The polymers obtained using $[Sn(Oct)_2]$ consistently gave higher molecular weights than those obtained using **1** and **2** under the same conditions. MALDI-ToF spectra for the PCL obtained via the use of $[Sn(Oct)_2]$ revealed the products to be mostly linear polymers with H/OH end groups (e.g., see Figure 6). At ambient temperature (15 °C), all complexes exhibited little or no activity.

Table 1. The ROP of ϵ -CL over 24 h catalysed by **1**, **2** $[Sn(Oct)_2]$, and $[Sn(OctBu)_4]$.

Entry	Cat.	[CL]:[Cat]	T/°C	Conv ^a (%)	$M_{n(obsv)}$ ^b	M_n Corrected ^c	$M_{n,Cal}$ ^d	\bar{D} ^b
1	1	500:1	130	>99	19,330	10,840	56,520	4.95
2 ^e	1	500:1	130	>99	9150	5140	56,250	1.84
3	1	1000:1	130	91	87,060	48,750	103,890	3.81
4 ^e	1	1000:1	130	81	16,300	9130	92,470	1.64
5	1	100:1	130	97	20,210	11,320	11,090	2.28
6 ^e	1	100:1	130	99	7460	4180	11,320	1.87
7 ^f	1	500:1	130	>99	18,300	10,250	56,520	2.15
8 ^{e,f}	1	500:1	130	98	14,020	7850	55,950	1.80
9	1	250:1	130	90	39,410	22,070	25,700	2.01
10 ^{e,f}	1	250:1	130	>99	13,840	7750	28,270	3.44
11 ^f	1	250:1	130	>99	70,370	39,410	28,270	2.01
12	1	500:1	15	0	-	-	-	-
13 ^e	1	500:1	15	0	-	-	-	-
14	2	500:1	130	>99	47,700	26,710	56,520	1.75
15 ^e	2	500:1	130	>99	38,880	21,770	56,520	1.48
16 ^f	2	500:1	130	91	27,580	15,440	51,950	2.02
17 ^{e,f}	2	500:1	130	99	9570	5360	56,520	2.00
18	2	500:1	15	44	-	-	-	-
19 ^e	2	500:1	15	18	-	-	-	-
20	Sn(Oct)₂	500:1	130	99	55,530	31,100	56,520	1.91
21 ^e	Sn(Oct)₂	500:1	130	56	10,730/3440	6010/1930	31,980	1.21/1.11
22	Sn(Oct)₂	500:1	130	92	21,120	11,830	52,520	2.31
23 ^{e,f}	Sn(Oct)₂	500:1	130	>99	10,920	6120	56,520	1.64
24	Sn(Oct)₂	500:1	15	0	-	-	-	-
25 ^e	Sn(Oct)₂	500:1	15	2	-	-	-	-
26	Sn(OctBu)₄	500:1	15	0	-	-	-	-
27 ^e	Sn(OctBu)₄	500:1	15	0	-	-	-	-
28	Sn(OctBu)₄	500:1	130	>99	57,940	32,450	56,520	7.81
29 ^f	Sn(OctBu)₄	500:1	130	99	124,070	69,480	56,520	23.9

^a Determined by ¹H NMR spectroscopy. ^b Measured by GPC in THF relative to polystyrene standards; ^c M_n calculated values after Mark-Houwink correction [53,54]; M_n corrected = $0.56 \times M_n$ obsd. ^d Calculated from $([CL]_0/[cat]_0) \times \text{conv} (\%) \times \text{monomer molecular weight} (M_{CL} = 114.14) + \text{end groups (H/OH used in this case)}$. ^e Conducted in air. ^f Conducted as a melt.

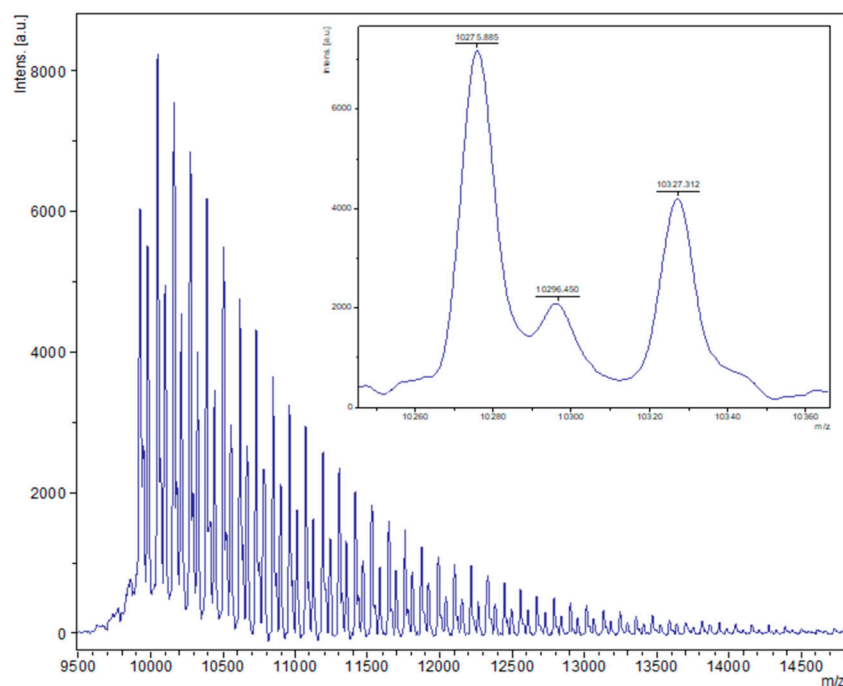


Figure 3. MALDI-ToF spectrum of PCL obtained from entry 4, Table 1 (1, 1000:1, melt, air). The main families are (i) chain polymer (terminated by 2 OH groups) as potassium adducts $[M = 17(\text{OH}) + 1(\text{H}) + n \times 114.14(\text{CL}) + 39.1(\text{K}^+)]$, e.g., for $n = 90$, calc. 10,329.7 obsv. 10,327.3; (ii) cyclic polymers as the sodium adducts $[M = n \times 114.14(\text{CL}) + 22.99(\text{Na}^+)]$, e.g., calc. 10,295.6, $n = 90$, obsv. 10,296.5.

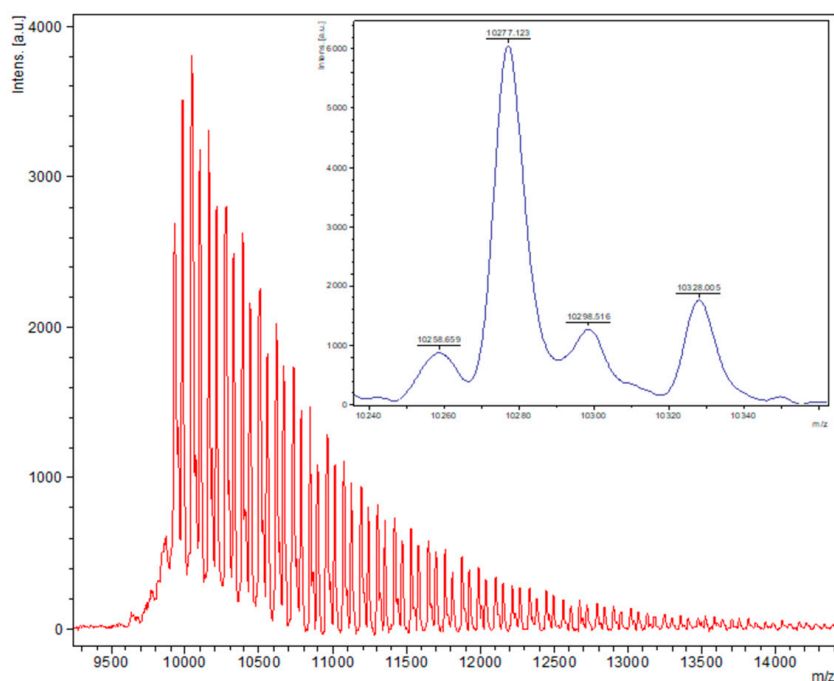


Figure 4. MALDI-ToF spectrum of PCL obtained from entry 7, Table 1 (1, 500:1 melt, N_2). The main families are (i) chain polymer (terminated by 2 OH groups) as potassium adducts $[M = 17(\text{OH}) + 1(\text{H}) + n \times 114.14(\text{CL}) + 39.1(\text{K}^+)]$, e.g., for $n = 90$, calc. 10,329.7 obsv. 10,328.0; (ii) cyclic polymers as the sodium adducts $[M = n \times 114.14(\text{CL}) + 22.99(\text{Na}^+)]$, e.g., calc. 10,295.6, $n = 90$, obsv. 10,298.5.

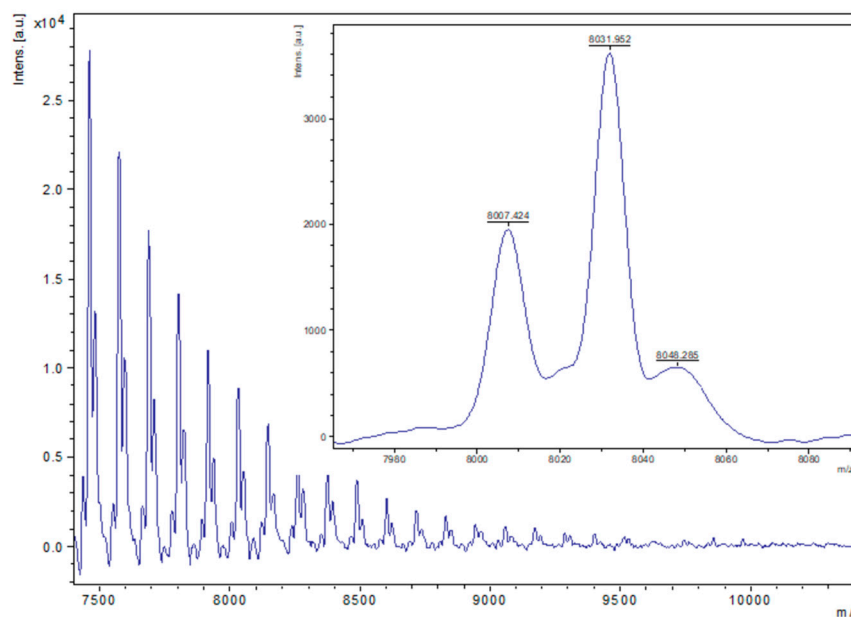


Figure 5. MALDI-ToF spectrum of PCL obtained from entry 16, Table 1 (2, 500:1 melt, air). The main families are (i) chain polymer (terminated by 2 OH groups, i.e., $\text{HO}(\text{C}_6\text{H}_{10}\text{O}_2)\text{H}$) [$M = 17 (\text{OH}) + 1(\text{H}) + n \times 114.14 (\text{CL}) + 22.99 (\text{Na}^+)$], e.g., for $n = 70$, calc. 8007.8 obsv. 8007.4; (ii) chain polymer (terminated by 2 OH groups) as sodium adducts [$M = 17 (\text{OH}) + 1(\text{H}) + n \times 114.14 (\text{CL}) + 22.99 (\text{Na}^+)$], e.g., for $n = 70$, calc. 8030.8 obsv. 8032.0. (iii) A minor family can be assigned to chain polymers terminated by OMe/OH end groups as sodium adducts [$M = 31 (\text{OMe}) + 1(\text{H}) + n \times 114.14 (\text{CL}) + 22.99 (\text{Na}^+)$], e.g., calc. 8044.8, $n = 70$, obsv. 8048.3.

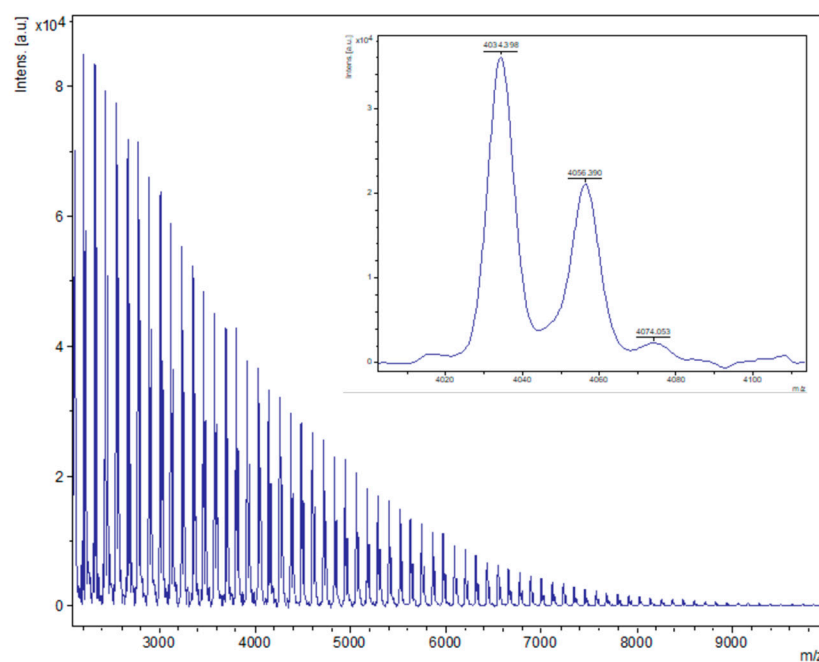


Figure 6. MALDI-ToF spectrum of PCL obtained from entry 22, Table 1 ($[\text{Sn}(\text{Oct})_2]$, 500:1 melt, air). The main family is a chain polymer (terminated by 2 OH groups) as sodium adducts [$M = 17 (\text{OH}) + 1(\text{H}) + n \times 114.14 (\text{CL}) + 22.99 (\text{Na}^+)$], e.g., for $n = 35$, calc. 4034.4 obsv. 4034.4; $n = 70$, calc. 8030.8 obsv. 8029.3.

A kinetic study (Figure 7) conducted using 500:1 ($[\epsilon\text{-CL}]:[\text{cat}]$) at 110 °C revealed the rate trend $[\text{Sn}(\text{Oct})_2] > \mathbf{1} > \mathbf{2} > [\text{Sn}(\text{OtBu})_4]$. Both $[\text{Sn}(\text{Oct})_2]$ and $\mathbf{1}$ are rather sluggish over the first 15 h (about 25 h for $\text{Sn}(\text{OtBu})_4$), consistent with a structural change under these

conditions to a more active species. For the individual kinetic traces, see Figures S12–S15 in the Supplementary Materials.

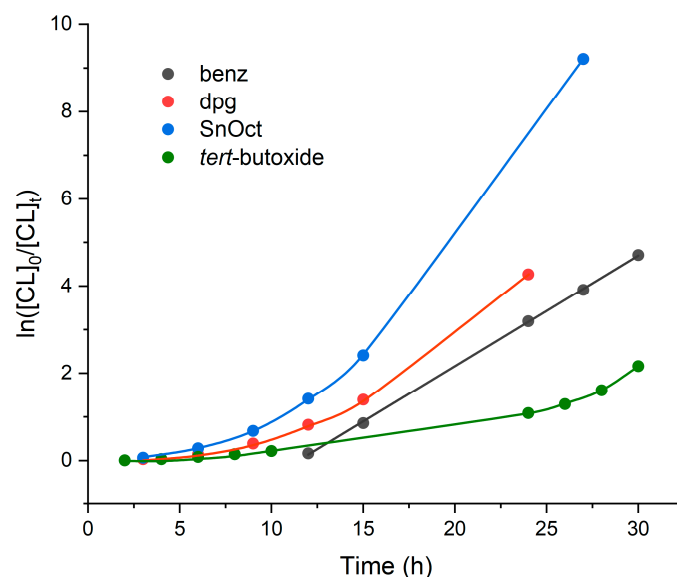


Figure 7. Kinetic runs using $[\epsilon\text{-CL}]:[\text{cat}] = 500:1$ at $110\text{ }^\circ\text{C}$ in toluene.

We note that during metal-free studies, we observed that benzoic acid was active for the ROP of $\epsilon\text{-CL}$ with near quantitative conversions when using high-catalyst loadings (20:1) at $150\text{ }^\circ\text{C}$ over 24 h, whereas for diphenylglycine, conversions were $\leq 5\%$ at $150\text{ }^\circ\text{C}$ over 24 h, with or without BnOH present [41].

3.2. Ring Opening Polymerization of $\delta\text{-Valerolactone}$ ($\delta\text{-VL}$)

Based on the $\epsilon\text{-CL}$ results, the complexes were screened for the ROP of $\delta\text{-VL}$ using the ratio of $[\text{VL}]:[\text{catalyst}]$ of 500:1 (Table 2). All complexes were found to be active under these polymerization conditions with monomer conversions ($\geq 77\%$), affording relatively low to moderate-molecular weight polymers; selected GPC traces are given in the Supplementary Materials (Figures S16–S23). Even at ambient temperature, **1**, **2**, $\text{Sn}(\text{Oct})_2$, and $[\text{Sn}(\text{OtBu})_4]$ were capable of the ROP of $\delta\text{-VL}$ with good conversions. This behaviour contrasts with previous ROP studies, where more robust conditions are usually needed for the ROP of $\delta\text{-VL}$ versus $\epsilon\text{-Cl}$ [38,39], and it is inconsistent with the thermodynamic parameters for these lactones [55].

Table 2. The ROP of $\delta\text{-VL}$ over 24 h catalysed by **1**, **2** $[\text{Sn}(\text{Oct})_2]$, and $[\text{Sn}(\text{OtBu})_4]$.

Entry	Cat.	$[\text{VL}]:[\text{Cat}]$	$T/^\circ\text{C}$	Conv ^a (%)	M_n^b	$M_n^{\text{corrected}}$	$M_{n,\text{Cal}}^c$	\bar{D}^d
1	1	500:1	15	81	4400	2510	40,570	1.60
2 ^e	1	500:1	15	80	3540	2020	40,070	2.57
3	1	500:1	130	>99	7190	4100	49,580	3.24
4 ^e	1	500:1	130	>99	13240	7540	49,580	1.07
5 ^f	1	500:1	130	93	17,390/3200	9910/1820	46,570	1.29/1.39
6 ^{e,f}	1	500:1	130	>99	5210	2970	49,580	1.61
7	2	500:1	130	88	16,060/3560	9150/2050	44,070	1.17/1.38
8 ^e	2	500:1	130	>99	13,540	7720	49,580	1.60
9 ^f	2	500:1	130	94	6040	3380	47,070	2.20
10 ^{e,f}	2	500:1	130	99	9560	5450	49,580	2.14
11	2	500:1	15	78	3660	2090	39,060	2.39

Table 2. Cont.

Entry	Cat.	[VL]:[Cat]	T/°C	Conv ^a (%)	M _n ^b	M _n corrected	M _{n,Cal} ^c	Đ ^d
12 ^e	2	500:1	15	77	2860	1630	38,560	2.15
13	Sn(Oct)₂	500:1	130	>99	8710	4960	49,580	1.99
14 ^e	Sn(Oct)₂	500:1	130	>99	8040	4580	49,580	1.65
15 ^f	Sn(Oct)₂	500:1	130	90	4130	2350	45,070	9.78
16 ^{e,f}	Sn(Oct)₂	500:1	130	>99	6620	3770	49,580	2.15
17	Sn(Oct)₂	500:1	15	89	2740	1560	44,570	1.89
18 ^e	Sn(Oct)₂	500:1	15	88	2450	1400	44,070	1.47
19	Sn(OtBu)₄	500:1	15	68	7540/4220	4300/2410 [§]	34,060	1.03/1.02
20 ^e	Sn(OtBu)₄	500:1	15	51	2810/1640	1600/930	25,550	1.03/1.03
21	Sn(OtBu)₄	500:1	130	>99	77,970	44,440	49,580	4.27
22 ^f	Sn(OtBu)₄	500:1	130	>99	38,890	22,170	49,580	2.96

^a Determined by ¹H NMR spectroscopy. ^b Measured by GPC in THF relative to polystyrene standards; ^c M_n calculated values after Mark–Houwink correction [53,54]; M_n corrected = 0.57 × M_n obsd. ^d Calculated from ([VL]₀/[cat]₀) × conv (%) × monomer molecular weight (M_{VL} = 100.12) + end groups (H/OH used in this case). ^e Conducted in air. ^f Conducted as a melt. [§] Lower M_n^b peaks were also observed at 2480 (Đ 1.02) and 1380 (Đ 1.04).

¹H NMR and mass spectra of the PVL again indicated that the products contained both linear and cyclic species. The MALDI-TOF spectra revealed several families of products, including H/OH- and H/OMe-terminated polymers and cyclic polymers (e.g., Figures 8–10; expansions are given as inserts). As for PCL, there was evidence of transesterification, and all observed PVL M_n values were significantly lower than the calculated values.

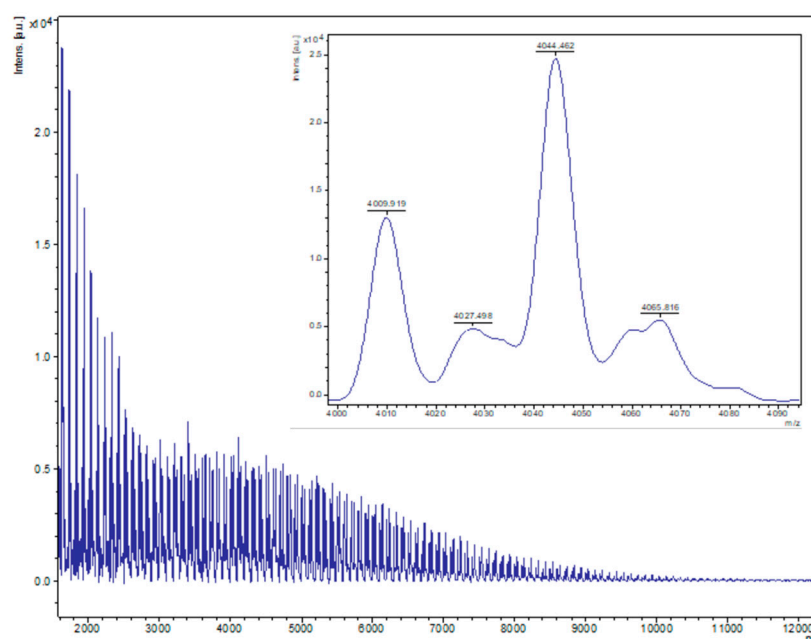


Figure 8. MALDI-ToF spectrum of PVL obtained from entry 3, Table 2 (1, 500:1, toluene, N₂). The main family is composed of chain polymers (terminated by 2 OH groups) as sodium adducts [M = 17 (OH) + 1(H) + n × 114.14 (CL) + 22.99 (Na⁺)], e.g., for n = 40, calc. 4046.6, obsv. 4044.5.

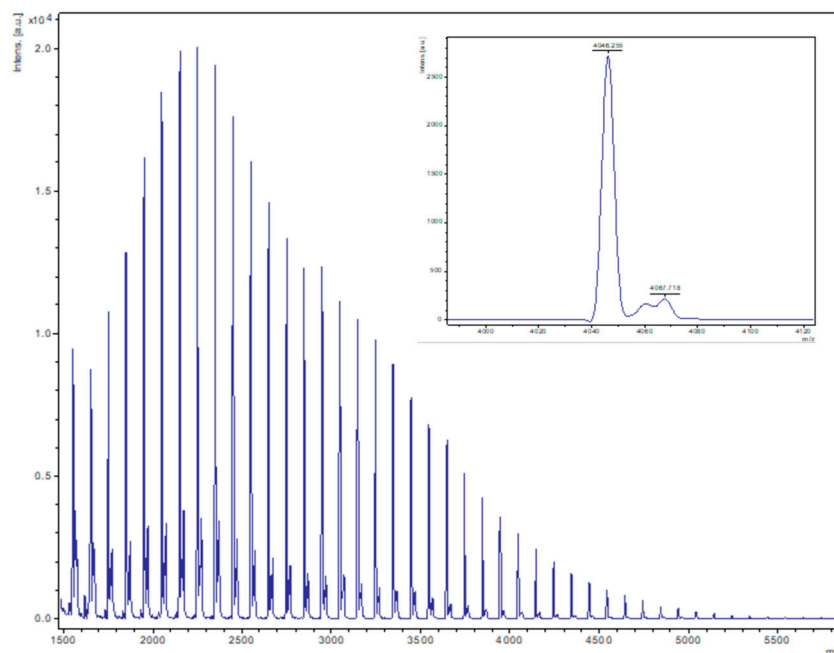


Figure 9. MALDI-ToF spectrum of PVL obtained from entry 10, Table 2 (2, 500:1 melt, N_2). The main family is composed of chain polymers (terminated by 2 OH groups) as sodium adducts [$M = 17$ (OH) + 1(H) + $n \times 114.14$ (CL) + 22.99 (Na^+)], e.g., for $n = 40$, calc. 4046.6 obsv. 4046.3.

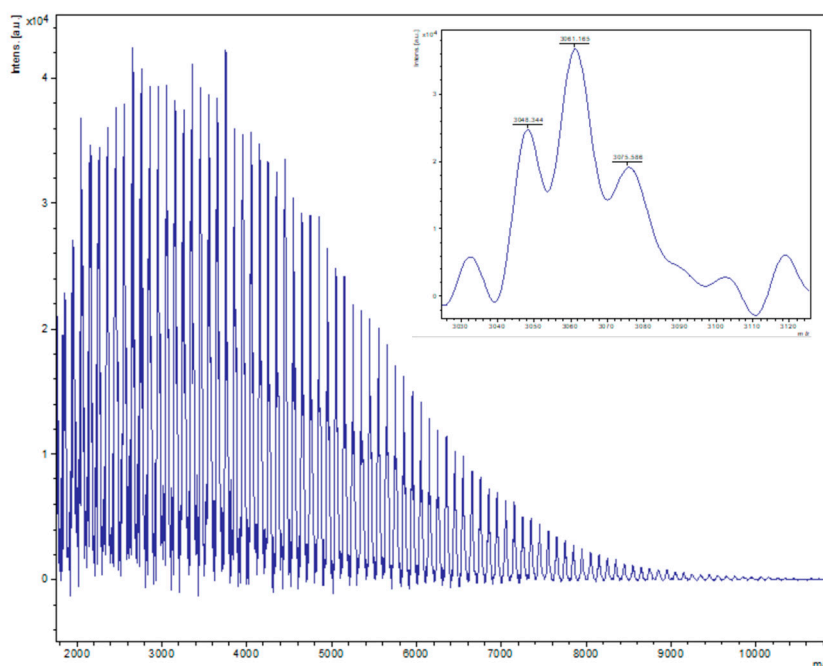


Figure 10. PVL obtained from entry 10, Table 2 (2, 500:1 melt, air). The main family is composed of chain polymers (terminated by OH/OMe groups) as sodium adducts [$M = 17$ (OH) + 1(H) + $n \times 114.14$ (CL) + 22.99 (Na^+)], e.g., for $n = 30$, calc. 3059.2, obsv. 3061.2.

A kinetic study (Figure 11) conducted using 500:1 ($[\epsilon\text{-CL}]:[\text{cat}]$) at 110 °C revealed the rate trend $[\text{Sn}(\text{Oct})_2] > 1 > [\text{Sn}(\text{O}t\text{Bu})_4] > 2$. In this case, sluggish behaviour is only observed for **1** over about 12 h and, as in the case of $\epsilon\text{-CL}$, for $\text{Sn}(\text{O}t\text{Bu})_4$ over about 25 h. For the individual kinetic traces, see Figures S24–S27 in the Supplementary Materials.

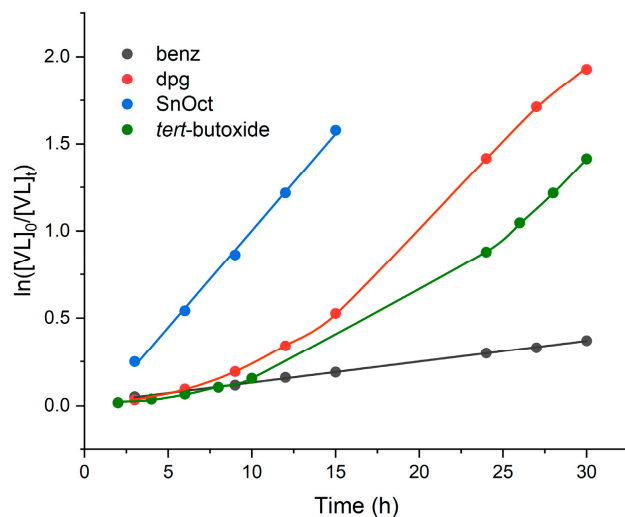


Figure 11. Kinetic runs using $[\delta\text{-VL}]:[\text{cat}] = 500:1$ at $110\text{ }^\circ\text{C}$ in toluene.

4. TGA Measurements

The stability of the complexes at the polymerization temperature was checked by TGA. The runs indicated that both systems were stable, and in the case of 1:2MeCN, only solvent of crystallization (MeCN) was lost (with calc./obsv. values of $\sim 7\%$) (see Figure 12).

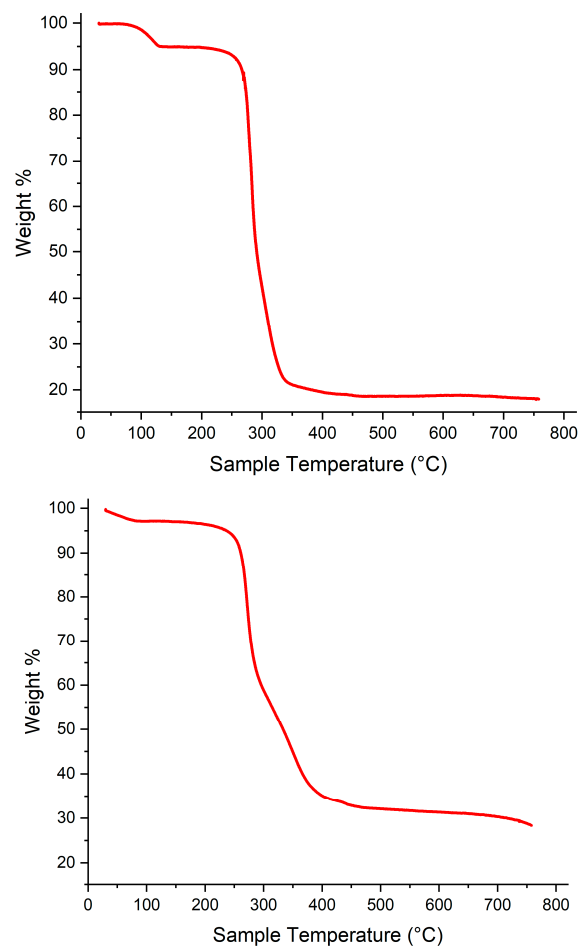


Figure 12. TGAs of top 1:2MeCN and bottom 2.

5. Materials and Methods

All manipulations were carried out under an atmosphere of nitrogen using standard Schlenk line and cannula techniques or a conventional N₂-filled glove box. Solvents were refluxed over the appropriate drying agents and distilled and degassed prior to use, i.e., toluene was refluxed over Na; acetonitrile was refluxed over calcium hydride. These were purchased from commercial sources and used directly. ϵ -Caprolactone (Fisher Scientific, Loughborough, UK) and δ -valerolactone (Sigma Aldrich, Gillingham, UK) were dried over CaH₂ and then distilled. Tin *tert*-butoxide (Sigma Aldrich, UK) was stored under nitrogen in a dry box. 2,2'-diphenylglycine (Sigma Aldrich, UK) and benzoic acid (Sigma Aldrich, UK) were dried under vacuum at 80 °C for 4 h prior to use. Elemental analyses were performed at the London Metropolitan University or Xi'an Rare Metal Materials Research Institute Co., Ltd. (Xi'an, China). FTIR spectra (nujol mulls, KBr windows) were recorded on a Nicolet Avatar 360 FT-IR spectrometer. ¹H NMR spectra were recorded at 400.2 MHz on a JEOL ECZ 400S spectrometer (Peabody, MA, USA), with TMS $\delta_{\text{H}} = 0$ as the internal standard or residual protic solvent; chemical shifts are given in ppm (δ). Matrix-Assisted Laser Desorption/Ionization–Time of Flight (MALDI-TOF) mass spectrometry was performed on a Bruker III smart beam in linear mode. MALDI-TOF mass spectra were acquired by averaging at least 100 laser shots. Molecular weights were calculated from the experimental traces using the OmniSEC software (Malvern Panalytical Ltd., Malvern, UK, v11.35). For the TGA runs, data were collected on a PerkinElmer TGA 400 (Shelton, CT, USA) using Pyris™ software (v11.0) and a rate of 10 °C per min over the 30 °C to 800 °C under N₂. Sample weights were typically between 3 and 5 mg.

5.1. Synthesis of $\{Sn[Ph_2C(NH_2)(CO_2)]_4\} \cdot 2MeCN$ (**1**·2MeCN)

Ph₂C(NH₂)CO₂H (1.00 g, 4.40 mmol) and Sn(O*t*Bu)₄ (0.90 g (0.85 mL), 2.20 mmol) were refluxed in toluene (20 mL) for 12 h. On cooling, the volatiles were removed in vacuo, and the residue was extracted into warm MeCN (30 mL). Removal of the MeCN afforded a white solid. Yield: 1.02 g, 84% (based on dpGH). C₅₆H₄₈N₄O₈Sn·2MeCN requires C 65.17, H 4.92, N 7.60%. Found C 65.26, H 4.89, N 7.71%. IR: 3406w, 3185w, 2357w, 2336w, 1958w, 1867w, 1659m, 1575s, 1489m, 1403s, 1318m, 1277m, 1261s, 1209w, 1169m, 1158m, 1094s, 1029s, 941w, 918w, 895m, 803s, 764m, 721m, 699s, 676w, 638m. M.S. 1023 (M⁺–2MeCN). ¹H NMR (CDCl₃) δ : 7.21 (bs, 40H, arylH), 3.45 (bs, 8H, NH₂), 1.96 (s, 6H, MeCN).

5.2. Synthesis of $\{Sn[Ph_2C(O)(CO_2)]_2(CH_3CO_2H)_2\}$ (**2**)

Ph₂C(OH)CO₂H (1.00 g, 4.38 mmol) and Sn(O*t*Bu)₄ (0.60 g, 1.46 mmol) were refluxed in toluene (20 mL) for 12 h. On cooling, the volatiles were removed in vacuo, and the residue was extracted into warm MeCN (30 mL). Removal of the MeCN afforded a white solid. Yield: 0.92 g, 91% (based on Sn). C₃₂H₂₈O₁₀Sn requires C 55.60, H 4.08%. Found C 55.14, H 3.93%. IR: 1957w, 1881w, 1810w, 1650s, 1560s, 1300s, 1281s, 1210m, 1164s, 1085m, 1047s, 1029s, 1002m, 985m, 940w, 906m, 822m, 783m, 758m, 723s, 698m, 621w. M.S. 404 (M⁺—acetic acid—doubly deprotonated benzoic acid). ¹H NMR (CDCl₃) δ : 7.63 (dd, 1H, J 8.0 Hz, J' 2.4 Hz, arylH), 7.51–7.41 (overlapping m, 7H, arylH), 7.33 (bm, 8H, arylH), 7.17 (bm, 2H, arylH), 7.05 (bm, 2H, arylH), 1.85 (bs, 2H, OH), 1.26 (s, 6H, Me).

5.3. ROP of ϵ -Caprolactone (ϵ -CL) and δ -Valerolactone (δ -VL)

The pre-catalyst (0.010 mmol) was added to a Schlenk tube in the glovebox at room temperature. For ROPs in solution, toluene (5 mL) was added. The appropriate amount of ϵ -CL (or δ -VL) was added, and the reaction mixture was then placed into a sand bath pre-heated at 130 °C and heated for the prescribed time (24 h) under either N₂ or air. The polymerization mixture was quenched on addition of an excess of glacial acetic acid

(0.2 mL) in methanol (50 mL). The resultant polymer was then collected on filter paper and dried in vacuo. GPC (in THF) were used to determine molecular weights (M_n and \bar{D}) of the polymer products.

5.4. Kinetic Studies

The polymerizations were carried out at 110 °C in toluene (2 mL) using 0.010 mmol of complex. The molar ratio of monomer to initiator to co-catalyst was fixed at 500:1, and at appropriate time intervals, 0.5 μ L aliquots were removed (under N_2) and were quenched with wet $CDCl_3$. The percent conversion of monomer to polymer was determined using 1H NMR spectroscopy.

5.5. X-Ray Crystallography

In both cases, crystals suitable for an X-ray diffraction study were grown from a saturated MeCN solution at 0 °C. Single crystal X-ray diffraction data were collected by the UK National Crystallography Service (NCS, Southampton, UK) using a Rigaku Oxford Diffraction diffractometer operating with a rotating anode X-ray generator and HyPix 6000HE detector (Neu-Isenberg, Germany). Table 3 contains basic crystallographic data and refinements details. It happens that one structure was collected using a Cu source and one with a Mo source; this normally reflects which instrument is available at the NCS at the time the sample is studied. There are not technical reasons for the different choice of sources. Samples were mounted on Mitegen loops and held at 100 K using an Oxford Cryosystems nitrogen gas cryostream. Both structures were solved and refined routinely [56–58]. H atoms were included in a riding model; $U_{iso}(H)$ was set to 120% of that of the carrier atoms except for OH, NH_3 , and CH_3 (150%). Further details are presented in Table 2. CCDC 2410598-9 contains the supplementary crystallographic data for this paper. These data can be obtained free of charge from the Cambridge Crystallographic Data Centre via www.ccdc.cam.ac.uk/structures (accessed on 10 January 2025).

Table 3. Crystallographic data for 1·2MeCN and 2.

Compound	1·2MeCN	2
Formula	$C_{64}H_{54}N_6O_8Sn$	$C_{32}H_{28}O_{10}Sn$
Formula weight	1105.78	691.23
Crystal system	Triclinic	Tetragonal
Space group	$P\bar{1}$	I-42d
Unit cell dimensions		
a (Å)	14.8890(3)	21.0627(5)
b (Å)	14.9289(3)	21.0627(5)
c (Å)	15.0152(3)	14.9499(5)
α (°)	114.697(2)	90
β (°)	104.025(2)	90
γ (°)	108.449(2)	90
V (Å ³)	2590.53(10)	6632.3(4)
Z	2	8
Temperature (K)	100(2)	100(2)
Wavelength (Å)	0.71075	1.54184
Calculated density (gcm ⁻³)	1.418	1.385
Absorption coefficient (mm ⁻¹)	0.557	6.578
Crystal size (mm ³)	0.10 × 0.07 × 0.03	0.25 × 0.20 × 0.12
θ (max) (°)	61.0	140.0

Table 3. Cont.

Compound	1·2MeCN	2
Reflections measured	66,619	43,429
Unique reflections	15,748	3162
R_{int}	0.056	0.086
Number of parameters	686	195
$R_1 [F^2 > 2\sigma(F^2)]$	0.049	0.074
wR_2 (all data)	0.131	0.16
GOOF, S	1.05	1.21
Largest difference peak and hole ($e \text{ \AA}^{-3}$)	2.61 and -0.61	0.65 and -1.10

6. Conclusions

In conclusion, the use of the acids $\text{Ph}_2\text{C}(\text{X})\text{CO}_2\text{H}$ on reaction with tin *tert*-butoxide afforded the complexes $\{\text{Sn}[\text{Ph}_2\text{C}(\text{NH}_2)(\text{CO}_2)]_4\} \cdot 2\text{MeCN}$ (1·2MeCN) for $\text{X} = \text{NH}_2$ or the complex $\{\text{Sn}[\text{Ph}_2\text{C}(\text{O})(\text{CO}_2)]_2(\text{CH}_3\text{CO}_2\text{H})_2\}$ (2) for $\text{X} = \text{OH}$. These tin-based systems are active as catalysts for the ROP of ϵ -caprolactone and δ -valerolactone when employed in solution (toluene) or as melts under either air or N_2 . The products are of low to high molecular weight for PCL (1150–48,750 Da) and low to moderate molecular weight for PVL (1630–7720 Da), generally with broad Đ (1.48–3.81 for PCL; 1.29–3.24 for PVL). A number of families were evident in the MALDI-ToF mass spectra, with polymers present assigned to those terminated with H/OH, H/OMe, and cyclic polymers. Kinetic profiles indicated that $[\text{Sn}(\text{Oct})_2]$ outperformed 1 and 2, though under certain conditions, 1 and 2 afforded high-molecular weight products with better control.

Supplementary Materials: The following supporting information can be downloaded at <https://www.mdpi.com/article/10.3390/catal15030261/s1>, Figure S1. An alternative view of 1·2MeCN. Figure S2. An alternative view of 2. Figures S3 and S4. ^1H NMR spectra of 1·2MeCN and 2. Figures S5–S11. Selected gpc traces for PCL. Figures S12–S15. Kinetic profiles for PCL formation using 1, 2, $[\text{Sn}(\text{Oct})_2]$ and $[\text{Sn}(\text{OtBu})_4]$. Figures S16–S23. Selected gpc traces for PVL. Figures S24–S27. Kinetic profiles for PVL formation using 1, 2, $[\text{Sn}(\text{Oct})_2]$ and $[\text{Sn}(\text{OtBu})_4]$.

Author Contributions: T.J.P.: Investigation, writing—review and editing. C.R.: Conceptualization, writing—original draft, writing—review and editing. All authors have read and agreed to the published version of the manuscript.

Funding: This research was funded by UKRI Creative Circular Plastic grant (EP/S025537/1).

Data Availability Statement: Data are contained within the article and Supplementary Materials.

Acknowledgments: CR thanks the EPSRC for support (grant no. EP/S025537/1). The EPSRC National Crystallographic Service Centre at Southampton University is thanked for data collection of 1·2MeCN and 2.

Conflicts of Interest: There are no conflicts of interest to declare.

References

1. Labet, M.; Thielemans, W. Synthesis of polycaprolactone: A review. *Chem. Soc. Rev.* **2009**, *38*, 3484–3504. [[CrossRef](#)] [[PubMed](#)]
2. Iwata, T. Biodegradable and Bio-Based Polymers: Future Prospects of Eco-Friendly Plastics. *Angew. Chem. Int. Ed.* **2015**, *54*, 3210–3215. [[CrossRef](#)] [[PubMed](#)]
3. Woodruff, M.A.; Hutmacher, D.W. The return of a forgotten polymer—Polycaprolactone in the 21st century. *Prog. Polym. Sci.* **2010**, *35*, 1217–1256. [[CrossRef](#)]
4. Thomas, C.M. Stereocontrolled ring-opening polymerization of cyclic esters: Synthesis of new polyester microstructures. *Chem. Soc. Rev.* **2010**, *39*, 165–173. [[CrossRef](#)]
5. Arbaoui, A.; Redshaw, C. Metal Catalysts for ϵ -caprolactone polymerisation. *Polym. Chem.* **2010**, *1*, 801–826. [[CrossRef](#)]

6. Sarazin, Y.; Carpentier, J.-F. Discrete Cationic Complexes for Ring-Opening Polymerization Catalysis of Cyclic Esters and Epoxides. *Chem. Rev.* **2015**, *115*, 3564–3614. [CrossRef]
7. Redshaw, C. Use of Metal Catalysts Bearing Schiff Base Macrocycles for the Ring Opening Polymerization (ROP) of Cyclic Esters. *Catalysts* **2017**, *7*, 165. [CrossRef]
8. Gao, J.; Zhu, D.; Zhang, W.; Solan, G.A.; Ma, Y.; Sun, W.-H. Recent progress in the application of group 1, 2 & 13 metal complexes as catalysts for the ring opening polymerization of cyclic esters. *Inorg. Chem. Front.* **2019**, *6*, 2619–2652. [CrossRef]
9. Lyubov, D.M.; Tolpygin, A.O.; Trifonov, A.A. Rare-earth metal complexes as catalysts for ring-opening polymerization of cyclic esters. *Coord. Chem. Rev.* **2019**, *392*, 83–145. [CrossRef]
10. Santoro, O.; Redshaw, C. Use of Titanium Complexes Bearing Diphenolate or Calix[*n*]arene Ligands in α -Olefin Polymerization and the ROP of Cyclic Esters. *Catalysts* **2020**, *10*, 210. [CrossRef]
11. Santoro, O.; Zhang, X.; Redshaw, C. Synthesis of biodegradable polymers: A review on the use of Schiff-base metal complexes as catalysts for the Ring Opening Polymerization (ROP) of cyclic esters. *Catalysts* **2020**, *10*, 800. [CrossRef]
12. Munzeiwa, W.A.; Omondi, B.O.; Nyamori, V.O. Perspective into ring-opening polymerization of ϵ -caprolactone and lactides: Effect of, ligand, catalyst structure and system dynamics, on catalytic activity and polymer properties. *Polym. Bull.* **2024**, *81*, 9419–9464. [CrossRef]
13. Available online: https://www.chemicalbook.com/ChemicalProductProperty_EN_CB0308694.htm (accessed on 14 January 2025).
14. Kowalski, A.; Duda, A.; Penczek, S. Kinetics and mechanism of cyclic esters polymerization initiated with Tin(II) Octoate, 1. Polymerization of ϵ -caprolactone. *Macromol. Rapid Commun.* **1998**, *19*, 567–572. [CrossRef]
15. Kricheldorf, H.R.; Kreiser-Saunders, I.; Sticker, A. Polylactones 48. SnOct₂-initiated polymerizations of lactide: A mechanistic study. *Macromolecules* **2000**, *33*, 702–709. [CrossRef]
16. Duda, A.; Penczek, S.; Kowalski, A.; Libiszowski, J. Polymerizations of ϵ -caprolactone and *L,L*-dilactide initiated with tin octoate and tin butoxide a comparison. *Macromol. Symp.* **2000**, *153*, 41–53. [CrossRef]
17. Byers, J.A.; Biernesser, A.B.; Delle Chiaie, K.R.; Kaur, A.; Kehl, J.A. Catalytic Systems for the Production of Poly(lactic acid). In *Synthesis, Structure and Properties of Poly(lactic acid)*; Springer: Cham, Switzerland, 2017; p. 67.
18. Kricheldorf, H.R.; Lee, S.R. Polylactones. 35. Macrocyclic and Stereoselective Polymerization of β -D,L-Butyrolactone with Cyclic Dibutyltin Initiators. *Macromolecules* **1995**, *28*, 6718–6725. [CrossRef]
19. Finne, A.; Albertsson, A.C. Controlled Synthesis of Star-Shaped L-Lactide Polymers Using New Spirocyclic Tin Initiators. *Biomacromolecules* **2002**, *3*, 684–690. [CrossRef]
20. Kricheldorf, H.R.; Fechner, B. Polylactones. 59. Biodegradable Networks via Ring-Expansion Polymerization of Lactones and Lactides with a Spirocyclic Tin Initiator. *Biomacromolecules* **2002**, *3*, 691–695. [CrossRef]
21. Storey, R.F.; Mullen, B.D.; Dsai, G.S.; Sherman, J.W.; Tang, C.N. Soluble tin(II) macroinitiator adducts for the controlled ring-opening polymerization of lactones and cyclic carbonates. *J. Polym. Sci. Part A Polym. Chem.* **2002**, *40*, 3434–3442. [CrossRef]
22. Kricheldorf, H.R.; Fechner, B. Polylactones. LVIII. Star-Shaped Polylactones with Functional End Groups via Ring-Expansion Polymerization with a Spiro initiator. *J. Polym. Sci. Part A Polym. Chem.* **2002**, *40*, 1047–1057. [CrossRef]
23. Odelius, K.; Finne, A.; Albertsson, A.C. Versatile and controlled synthesis of resorbable star-shaped polymers using a spirocyclic tin initiator—Reaction optimization and kinetics. *J. Polym. Sci. Part A Polym. Chem.* **2006**, *44*, 596–605. [CrossRef]
24. Odelius, K.; Albertsson, A.C. Precision synthesis of microstructures in star-shaped copolymers of ϵ -caprolactone, L-lactide, and 1,5-dioxepan-2-one. *J. Polym. Sci. Part A Polym. Chem.* **2008**, *46*, 1249–1264. [CrossRef]
25. Ma, W.-A.; Wang, Z.-X. Synthesis and characterisation of aluminium (III) and tin (II) complexes bearing quinoline-based *N,N,O*-tridentate ligands and their catalysis in the ring-opening polymerisation of ϵ -caprolactone. *Dalton Trans.* **2011**, *40*, 1778–1786. [CrossRef] [PubMed]
26. Phomphrai, K.; Pongchan-o, C.; Thumrongpatanaraks, W.; Sangtrirutnugul, P.; Kongsaree, P.; Pohmakotr, M. Synthesis of high-molecular-weight poly(ϵ -caprolactone) catalyzed by highly active bis(amidinate) tin(II) complexes. *Dalton Trans.* **2011**, *40*, 2157–2159. [CrossRef]
27. Piromjitpong, P.; Ratanapanee, P.; Thumrongpatanaraks, W.; Kongsaree, P.; Phomphrai, K. Synthesis of cyclic polylactide catalysed by bis(salicylaldiminato)tin(II) complexes. *Dalton Trans.* **2012**, *41*, 12704–12710. [CrossRef]
28. Lee, E.J.; Lee, K.M.; Jang, J.; Kim, E.; Chung, J.S.; Do, Y.; Yoon, S.C.; Park, S.Y. Characteristics of silica-supported tin(II) methoxide catalysts for ring-opening polymerization (ROP) of *L*-lactide. *J. Mol. Cat. A Chem.* **2014**, *385*, 68–72. [CrossRef]
29. Limwanich, W.; Khunmanee, S.; Kungwan, N.; Punyodom, W.; Meepowpan, P. Effect of tributyltin alkoxides chain length on the ring-opening polymerization of ϵ -caprolactone: Kinetics studies by non-isothermal DSC. *Thermochim. Acta* **2015**, *599*, 1–7. [CrossRef]
30. Punyodom, W.; Limwanich, W.; Meepowpan, P. Tin(II) *n*-butyl *L*-lactate as novel initiator for the ring-opening polymerization of epsilon-caprolactone: Kinetics and aggregation equilibrium analysis by non-isothermal DSC. *Thermochim. Acta* **2017**, *655*, 337–343. [CrossRef]

31. Praban, S.; Yimthachote, S.; Kiriratnikom, J.; Chotchatchawankul, S.; Tantirungrotechai, J.; Phomphrai, K. Synthesis and characterizations of bis(phenoxy)-amine tin(II) complexes for ring-opening polymerization of lactide. *J. Polym. Sci. Part A Polym. Chem.* **2019**, *57*, 2104–2112. [[CrossRef](#)]
32. Sriyai, M.; Chaiwon, T.; Molloy, R.; Meepowpan, P.; Punyodom, W. Efficiency of liquid tin(II) *n*-alkoxide initiators in the ring-opening polymerization of L-lactide: Kinetic studies by non-isothermal differential scanning calorimetry. *RSC Adv.* **2020**, *10*, 43566–43578. [[CrossRef](#)]
33. Kricheldorf, H.R.; Weidner, S.M. ROP of L-lactide and ϵ -caprolactone catalyzed by tin(II) and tin(IV) acetates—switching from COOH terminated linear chains to cycles. *J. Polym. Sci.* **2021**, *59*, 439–450. [[CrossRef](#)]
34. Kricheldorf, H.R.; Weidner, S.M. Syntheses of polylactides by means of tin catalysts. *Polym. Chem.* **2022**, *13*, 1618–1647. [[CrossRef](#)]
35. Novák, M.; Milasheuskaya, Y.; Srb, M.; Podzimek, S.; Bouška, M.; Jambor, R. Synthesis of star-shaped poly(lactide)s, poly(valerolactone)s and poly(caprolactone)s via ROP catalysed by N-donor tin(II) cations and comparison of their wetting properties with linear analogues. *RSC Adv.* **2024**, *14*, 23273–23285. [[CrossRef](#)] [[PubMed](#)]
36. Funfuenha, W.; Punyodom, W.; Meepowpan, P.; Limwanich, W. Microwave-assisted solvent-free ring-opening polymerization of ϵ -caprolactone initiated by *n*-butyltin(IV) chlorides. *Polym. Bull.* **2024**, *81*, 475–490. [[CrossRef](#)]
37. Prior, T.J.; Burke, B.P.; Roberts, D.P.; Archibald, S.J.; Stasiuk, G.; Higham, L.J.; Redshaw, C. Water-Soluble Rhenium Phosphine Complexes Incorporating the Ph₂C(X) Motif (X = O[−], NH[−]): Structural and Cytotoxicity Studies. *Inorg. Chem.* **2020**, *59*, 2367–2378. [[CrossRef](#)]
38. Al-Khafaji, Y.F.; Elsegood, M.R.J.; Frese, J.W.A.; Redshaw, C. Ring opening polymerization of lactides and lactones by multimetallic alkyl zinc complexes derived from the acids Ph₂C(X)CO₂H (X = OH, NH₂). *RSC Adv.* **2017**, *7*, 4510–4517. [[CrossRef](#)]
39. Wang, X.; Zhao, K.-Q.; Al-Khafaji, Y.F.; Mo, S.; Prior, T.J.; Elsegood, M.R.J.; Redshaw, C. Organoaluminium complexes derived from anilines or Schiff bases for the ring-opening polymerization of ϵ -caprolactone, δ -valerolactone and *rac*-lactide. *Eur. J. Inorg. Chem.* **2017**, *2017*, 1951–1965. [[CrossRef](#)]
40. Al-Khafaji, Y.F.; Prior, T.J.; Horsburgh, L.; Elsegood, M.R.J.; Redshaw, C. Ring opening polymerization of lactides and lactones by multimetallic lithium complexes derived from the acids Ph₂C(X)CO₂H (X = OH, NH₂). *Chem. Select* **2017**, *2*, 759–768. [[CrossRef](#)]
41. Collins, J.; Santoro, O.; Prior, T.J.; Chen, K.; Redshaw, C. Rare-earth metal complexes derived from the acids Ph₂C(X)CO₂H (X = OH, NH₂): Structural and ring opening polymerization (ROP) studies. *J. Mol. Struct.* **2021**, *1224*, 129083. [[CrossRef](#)]
42. Alshamrani, A.F.A.; Santoro, O.; Ounsworth, S.; Prior, T.J.; Stasiuk, G.J.; Redshaw, C. Synthesis, characterisation and ROP catalytic evaluation of Cu(II) complexes bearing 2,2′-diphenylglycine-derived moieties. *Polyhedron* **2021**, *195*, 114977. [[CrossRef](#)]
43. Zhang, X.; Prior, T.J.; Chen, K.; Santoro, O.; Redshaw, C. Ring opening polymerization of lactides and lactones by multimetallic titanium complexes derived from the acids Ph₂C(X)CO₂H (X = OH, NH₂). *Catalysts* **2022**, *12*, 935. [[CrossRef](#)]
44. Zhang, X.; Prior, T.J.; Redshaw, C. Niobium and Tantalum complexes derived from the acids Ph₂C(X)CO₂H (X = OH, NH₂): Synthesis, structure and ROP capability. *New J. Chem.* **2022**, *46*, 14146–14154. [[CrossRef](#)]
45. Glenister, M.A.; Frese, J.W.A.; Elsegood, M.R.J.; Canaj, A.B.; Brechin, E.; Redshaw, C. Reaction of Ph₂C(X)(CO₂H) (X = OH, NH₂) with [VO(OR)₃] (R = Et, *n*Pr): Structure, magnetic susceptibility and ROP capability. *Dalton Trans.* **2024**, *53*, 5351–5355. [[CrossRef](#)]
46. Braun, M. The “Magic” Diarylhydroxymethyl Group. *Angew. Chem.* **1996**, *35*, 519–522. [[CrossRef](#)]
47. Coxall, R.A.; Harris, S.G.; Henderson, D.K.; Parsons, S.; Tasker, P.A.; Winpenny, R.E.P. Inter-ligand reactions: In situ formation of new polydentate ligands. *J. Chem. Soc. Dalton Trans.* **2000**, 2349–2356. [[CrossRef](#)]
48. Etter, M.C.; MacDonald, J.C. Graph-Set Analysis of Hydrogen-Bond Patterns in Organic Crystals. *Acta Cryst.* **1990**, *B46*, 256–262. [[CrossRef](#)]
49. Delgado, G.E.; Mora, A.J.; Ramírez, B.; Díaz de Delgado, G.; Cisterna, J.; Cádenas, A.; Brito, I. Synthesis, Crystal Structure and Hirshfeld Surface Analysis of a new Coordination Polymer: Strontium Benzilate. *J. Chil. Chem. Soc.* **2021**, *66*, 5081–5085. [[CrossRef](#)]
50. March, J. *Advanced Organic Chemistry: Reactions, Mechanisms, and Structure*, 2nd ed.; McGraw-Hill, Inc.: New York, NY, USA, 1977.
51. Parris, C.L.; Christenson, R.M. N-Alkylation of Nitriles with Benzyl Alcohol, Related Alcohols, and Glycols. *J. Org. Chem.* **1960**, *25*, 331. [[CrossRef](#)]
52. Mo, J.; Zhang, X.; Zhao, N.; Xiao, F.; Wei, W.; Sun, Y. Mechanism of TBD-catalyzed hydrolysis of acetonitrile. *J. Mol. Struct. Theochem.* **2009**, *911*, 40–45. [[CrossRef](#)]
53. Huang, C.-H.; Wang, F.-C.; Ko, B.-T.; Yu, T.-L.; Lin, C.-C. Ring-Opening Polymerization of ϵ -Caprolactone and L-Lactide Using Aluminum Thiolates as Initiator. *Macromolecules* **2001**, *34*, 356–361. [[CrossRef](#)]
54. Save, M.; Schappacher, M.; Soum, A. Controlled Ring-Opening Polymerization of Lactones and Lactides Initiated by Lanthanum Isopropoxide, 1. General Aspects and Kinetics. *Macromol. Chem. Phys.* **2002**, *203*, 889–899. [[CrossRef](#)]
55. Dubois, P.; Coulembier, O.; Raquez, J.-M. (Eds.) *Handbook of Ring Opening Polymerization*; Wiley-VCH: Hoboken, NJ, USA, 2009; p. 594. [[CrossRef](#)]
56. Sheldrick, G.M. Crystal structure refinement with SHELXL. *Acta Cryst.* **2015**, *C71*, 3–8. [[CrossRef](#)]

57. Sheldrick, G.M. *SHELXT*—Integrated space-group and crystal-structure determination. *Acta Cryst.* **2015**, *A71*, 3–8. [[CrossRef](#)]
58. Palatinus, L.; Chapuis, G. SUPERFLIP—A computer program for the solution of crystal structures by charge flipping in arbitrary dimensions. *J. Appl. Cryst.* **2007**, *40*, 786–790. [[CrossRef](#)]

Disclaimer/Publisher’s Note: The statements, opinions and data contained in all publications are solely those of the individual author(s) and contributor(s) and not of MDPI and/or the editor(s). MDPI and/or the editor(s) disclaim responsibility for any injury to people or property resulting from any ideas, methods, instructions or products referred to in the content.